Acta Cryst E CRYSTALLOGRAPHIC COMMUNICATIONS

ISSN 2056-9890

Received 29 June 2020
Accepted 30 June 2020

Edited by W. T. A. Harrison, University of Aberdeen, Scotland

‡ Additional correspondence author, e-mail: kacrouse@gmail.com.

Keywords: crystal structure; Schiff base; hydrazine carbodithioate; hydrogen bonding; Hirshfeld surface analysis; DFT.

CCDC reference: 2013050

Supporting information: this article has supporting information at journals.iucr.org/e

2-[(1*E*)-[(*Z*)-2-({[(1*Z*)-[(*E*)-2-[(2-Hydroxyphenyl)-methylidene]hydrazin-1-ylidene]({[(4-methylphenyl)methyl]sulfanyl})methyl]disulfanyl}({[(4-methylphenyl)methyl]sulfanyl})methylidene)hydrazin-1-ylidene]methyl]phenol: crystal structure, Hirshfeld surface analysis and computational study

Georgiana Paulus,[a] Huey Chong Kwong,[a] Karen A. Crouse[a]‡ and Edward R. T. Tiekink[b]*

[a]Department of Chemistry, Faculty of Science, Universiti Putra Malaysia, UPM, Serdang 43400, Malaysia, and [b]Research Centre for Crystalline Materials, School of Science and Technology, Sunway University, 47500 Bandar Sunway, Selangor Darul Ehsan, Malaysia. *Correspondence e-mail: edwardt@sunway.edu.my

The complete molecule of the title hydrazine carbodithioate derivative, $C_{32}H_{30}N_4O_2S_4$, is generated by a crystallographic twofold axis that bisects the disulfide bond. The molecule is twisted about this bond with the C—S—S—C torsion angle of 90.70 (8)° indicating an orthogonal relationship between the symmetry-related halves of the molecule. The conformation about the imine bond [1.282 (2) Å] is *E* and there is limited delocalization of π-electron density over the CN_2C residue as there is a twist about the N—N bond [C—N—N—C torsion angle = −166.57 (15)°]. An intramolecular hydroxyl-O—H···N(imine) hydrogen bond closes an *S*(6) loop. In the crystal, methylene-C—H···π(tolyl) contacts assemble molecules into a supramolecular layer propagating in the *ab* plane: the layers stack without directional interactions between them. The analysis of the calculated Hirshfeld surfaces confirm the importance of H···H contacts, which contribute 46.7% of all contacts followed by H···C/C···H contacts [25.5%] reflecting, in part, the C—H···π(tolyl) contacts. The calculation of the interaction energies confirm the importance of the dispersion term and the influence of the stabilizing H···H contacts in the inter-layer region.

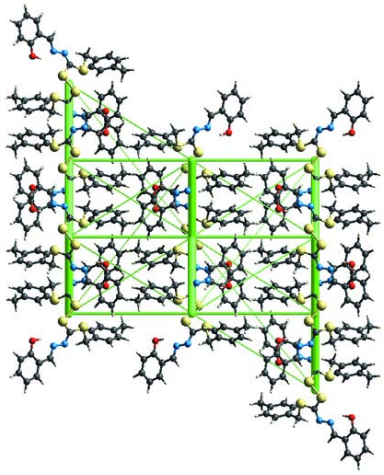

1. Chemical context

Schiff base molecules can be derived from the condensation of *S*-alkyl-dithiocarbazate derivatives with heterocyclic aldehydes and ketones to form molecules of the general formula $RSC(=S)N(H)N=C(R')R''$, where R', R'' = alkyl and aryl. These molecules are effective ligands for a variety of metals and the motivation for complexation largely stems from the promising biological activity exhibited by the derived metal complexes (Low *et al.*, 2016; Ravoof *et al.*, 2017; Yusof *et al.*, 2020). However, these Schiff bases are susceptible to oxidation resulting in the formation of a disulfide bond, as has been observed previously (Amirnasr *et al.*, 2014; Sohtun *et al.*, 2018). This is the case in the present report where the title compound, (I), was the side-product from the synthesis of the Schiff base, 4-methylbenzyl-2-(2-hydroxybenzylidene) hydrazinecarbodithioate (Ravoof *et al.*, 2010). After crystals of the desired Schiff base that had precipitated overnight were removed by filtration, the slow evaporation of the filtrate over a period of several days yielded crystals of (I). Herein, the

crystal and molecular structures of (I) are described along with an analysis of the calculated Hirshfeld surfaces and computation of interaction energies in the crystal.

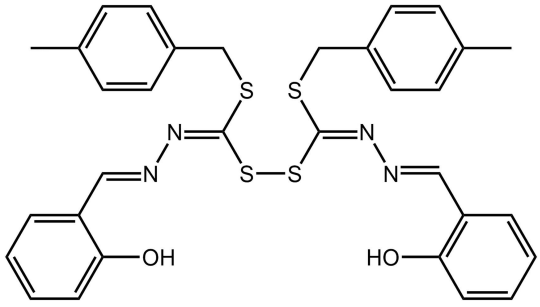

2. Structural commentary

The crystallographic asymmetric unit of (I) comprises half a molecule as it is disposed about a twofold axis of symmetry bisecting the disulfide bond, Fig. 1. The C1, N1, S1 and S2 atoms lie in a plane with an r.m.s. deviation of 0.0020 Å. The appended N2 and C5 atoms lie 0.036 (2) and 0.052 (2) Å to one side of the plane and the S1^{i} atom −0.1659 (16) Å to the other side; symmetry operation (i): $1-x, y, \frac{3}{2}-z$. The C1—S1 bond length of 1.7921 (17) Å is significantly longer than the C1—S2 bond of 1.7463 (17) Å, which is ascribed to the S1 atom participating in the S1—S1^{i} bond of 2.0439 (8) Å; each C1—S bond is shorter than the C9—S2 bond length of 1.8308 (18) Å.

The sequence of C1═N1 (*E*-conformation), N1—N2 and C2═N2 bond lengths is 1.282 (2), 1.409 (2) and 1.286 (2) Å, respectively, and suggests limited delocalization of π-electron density over this residue which is consistent with a twist about the N1—N2 bond as seen in the C1—N1—N2—C2 torsion angle of −166.57 (15)°. The presence of an intramolecular hydroxyl-O—H···N(imine) hydrogen bond, Table 1, is noted and accounts for the planarity in this region of the molecule as seen in the values of the N2—C2—C3—C4 and C2—C3—C4—O1 torsion angles of 3.8 (3) and 1.8 (3)°, respectively. The dihedral angle between the hydroxybenzene and tolyl rings is 65.11 (6)°, indicating a significant twist in this part of the molecule. Overall, the molecule is twisted about the central disulfide bond with the C1—S1—S1^{i}—C1^{i} torsion angle being 90.70 (8)° and the dihedral angle between the two CNS_2 planes being 88.22 (3)°.

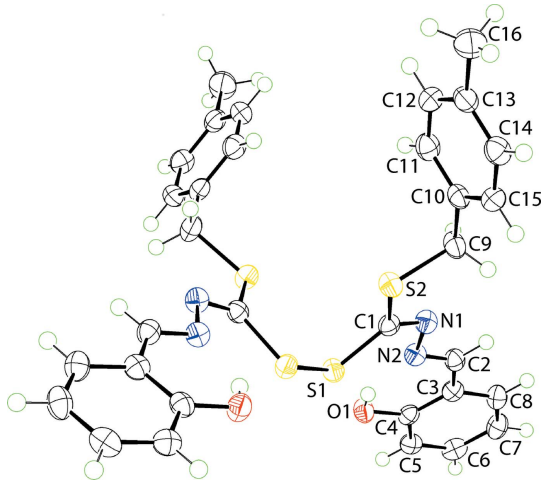

Figure 1
The molecular structure of (I) showing the atom-labelling scheme and displacement ellipsoids at the 70% probability level.

Table 1
Hydrogen-bond geometry (Å, °).

*Cg*1 is the centroid of the (C10–C15) ring.

D—H···*A*	*D*—H	H···*A*	*D*···*A*	*D*—H···*A*
O1—H1*O*···N2	0.84 (2)	1.94 (2)	2.6877 (19)	148 (2)
C9—H9*A*···*Cg*1^{i}	0.99	2.93	3.9075 (18)	169

Symmetry code: (i) $x, -y-1, z-\frac{1}{2}$.

3. Supramolecular features

In the crystal, the only directional contact identified in the geometric analysis of the molecular packing employing

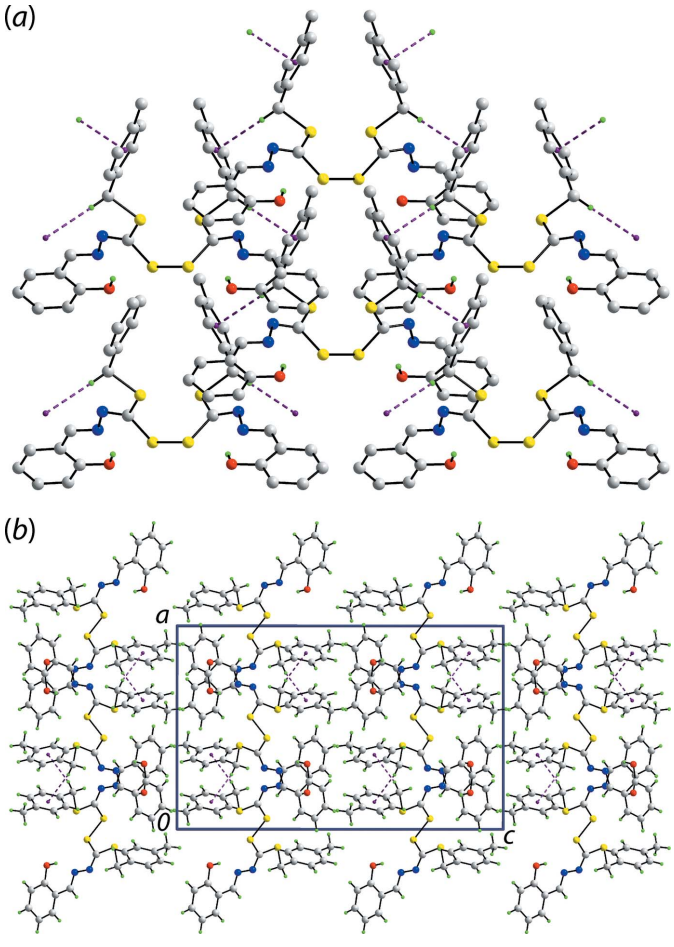

Figure 2
Molecular packing in (I): (*a*) the supramolecular layer in the *ab* plane sustained by methylene-C—H···π(tolyl) interactions shown as purple dashed lines (the non-participating H atoms removed for clarity) and (*b*) a view of the unit-cell contents shown in projection down the *b* axis highlighting the stacking of layers.

Table 2
A summary of short interatomic contacts (Å) for (I)[a].

Contact	Distance	Symmetry operation
C2···O1	3.07	$\frac{1}{2}-x,\frac{1}{2}+y,z$
C2···C4	3.25	$\frac{1}{2}-x,\frac{1}{2}+y+,z$
C12—H12···S1	2.82	$1-x,1+y+1,\frac{3}{2}-z$
C9—H9*B*···N1	2.59	$\frac{1}{2}-x,\frac{1}{2}+y,z$
C8—H8···C11	2.74	$-\frac{1}{2}+x,-\frac{1}{2}+y,\frac{3}{2}-z$
H6···H14	2.39	$\frac{1}{2}-x,\frac{1}{2}-y,\frac{1}{2}+z$

Note: (*a*) The interatomic distances are calculated in *Crystal Explorer 17* (Turner *et al.*, 2017) with the *X*—H bond lengths adjusted to their neutron values.

PLATON (Spek, 2020), is a methylene-C—H···π(tolyl) contact, Table 1. As each molecule donates and accepts two such contacts and these extend laterally, a supramolecular layer in the *ab* plane is formed, Fig. 2(*a*). Layers stack along the *c* axis without directional interactions between them, Fig. 2(*b*).

4. Analysis of the Hirshfeld surfaces

The Hirshfeld surface analysis comprising d_{norm} surface, electrostatic potential (calculated using wave function at the HF/STO-3 G level of theory) and two-dimensional fingerprint plot calculations were performed for (I) to quantify the interatomic interactions between molecules. This was accomplished using *Crystal Explorer 17* (Turner *et al.*, 2017) and following established procedures (Tan *et al.*, 2019). The bright-red spots on the Hirshfeld surface mapped over d_{norm} in Fig. 3(*a*), *i.e.* near the imine-C2 and tolyl ring, centroid designated *Cg*1, correspond to the C2···O1, C2···C4 short contacts (with separations ~0.15 Å shorter than the sum of their van der Waals radii, Table 2) and the methylene-C9—H9*A*···π(tolyl) interaction, Table 1. In addition, this methylene-C9—H9*A*···π(tolyl) interaction shows up as a distinctive orange 'pothole' on the shape-index-mapped Hirshfeld surface, Fig. 3(*b*).

In the views of Fig. 4(*a*), the faint red spots appearing near the tolyl-H12, methylene-H9*B* and phenol-H8 atoms correlate with the faint red spots near the sulfanyl-S1, hydrazine-N1 and tolyl-C11 atoms, and correspond to the intra-layer tolyl-C12—H12···S1(sulfanyl), methylene-C9—H9*B*···N1(hydrazine) and phenol-C8—H8···C11(tolyl) interactions, Table 2. These

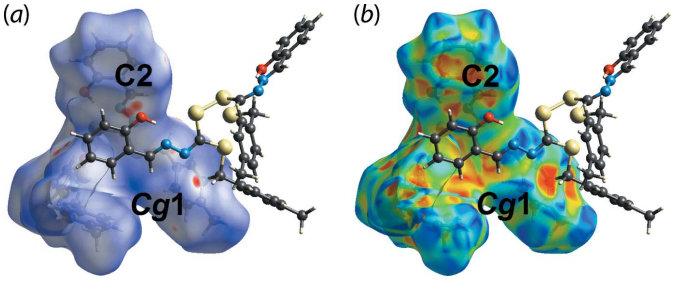

Figure 3
Views of the Hirshfeld surface for (I) mapped over (*a*) d_{norm} in the range −0.104 to + 1.517 arbitrary units and (*b*) the shape-index property.

Table 3
The percentage contributions of interatomic contacts to the Hirshfeld surface for (I).

Contact	Percentage contribution
H···H	43.9
H···C/C···H	25.5
H···S/S···H	13.6
H···O/O···H	5.7
N···C/C···N	3.6
H···N/N···H	3.4
O···C/C···O	1.7
C···C	1.2
S···C/C···S	1.0
N···N	0.4

interactions are also reflected in the Hirshfeld surface mapped over the calculated electrostatic potential in Fig. 4(*b*), with the blue and red regions corresponding to positive and negative electrostatic potentials, respectively.

The corresponding two-dimensional fingerprint plots for the calculated Hirshfeld surface of (I) are shown with characteristic pseudo-symmetric wings in the upper left and lower right sides of the d_e and d_i diagonal axes for the overall fingerprint plot, Fig. 5(*a*); those delineated into H···H, H···C/C···H, H···S/S···H, H···O/O···H, N···C/C···N and H···N/N···H contacts are illustrated in Fig. 5(*b*)–(*g*), respectively. The percentage contributions for the different interatomic contacts to the Hirshfeld surface are summarized in Table 3. The greatest contribution to the overall Hirshfeld surface is due to H···H contacts, which contribute 43.9% and features a round-shaped peak tipped at $d_e = d_i$ ~2.4 Å, Fig. 5(*b*). The tip of this H···H contact corresponds to an inter-layer H6···H14 contact with a distance of 2.39 Å, Table 2; the remaining H···H contacts are either around or longer than the sum of their van der Waals radii. The H···C/C···H contacts contribute 25.5% to the overall Hirshfeld surface, reflecting, in part,

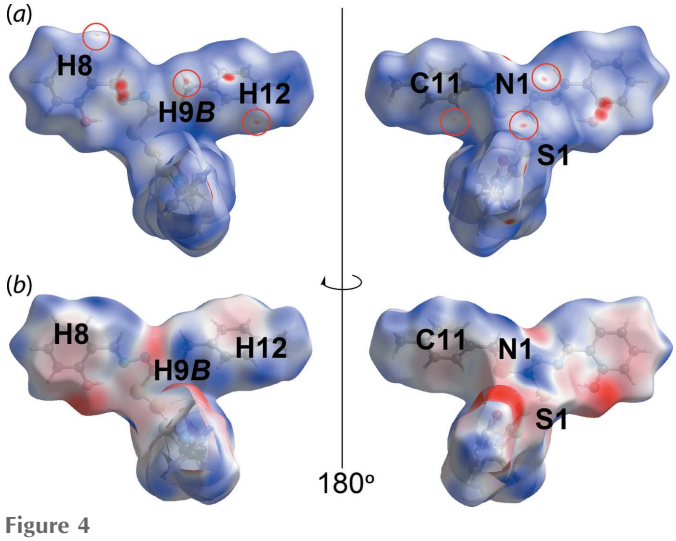

Figure 4
Views of the Hirshfeld surface mapped for (I) over (*a*) d_{norm} in the range −0.104 to + 1.517 arbitrary units and (*b*) the calculated electrostatic potential in the range −0.056 to 0.031 a.u. The red and blue regions represent negative and positive electrostatic potentials, respectively.

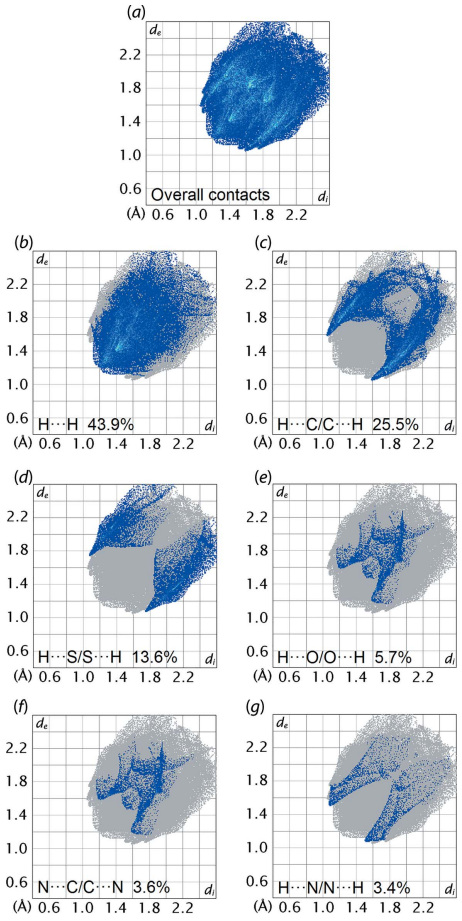

Figure 5
(*a*) A comparison of the full two-dimensional fingerprint plot for (I) and those delineated into (*b*) H···H, (*c*) H···C/C···H, (*d*) H···S/S···H, (*e*) H···O/O···H, (*f*) N···C/C···N and (*g*) H···N/N···H contacts.

the significant C—H···π interactions evident in the packing, Table 1. The shortest contacts are reflected as two spikes at $d_e + d_i$ ~2.7 Å in Fig. 5(*c*). The H···S/S···H contacts contribute 13.6% and appear as two sharp-symmetric wings at $d_e + d_i$ ~2.8 Å, Fig. 5(*d*). This feature reflects the intra-layer tolyl-C12—H12···S1(sulfanyl) interaction, Table 2. The H···O/O···H contacts contribute 5.7% and features forceps-like tips at $d_e + d_i$ ~2.8 Å, Fig. 5(*e*); this separation is ~0.08 Å longer than the sum of their van der Waals radii. Although both N···C/C···N and H···N/N···H contacts appear at $d_e + d_i$ ~2.6–2.8 Å in the respective fingerprint plots, Fig. 5(*f*) and (*g*), their contributions to the overall Hirshfeld surface are only 3.6 and 3.4%, respectively. The contributions from the other interatomic contacts summarized in Table 3 have an insignificant influence on the calculated Hirshfeld surface of (I).

Table 4
A summary of interaction energies (kJ mol^{-1}) calculated for (I).

Contact	R (Å)	E_{ele}	E_{pol}	E_{dis}	E_{rep}	E_{tot}
Intra-layer region						
C9—H9*A*···*Cg*1^{i} + C2···O1^{ii} + C2···C4^{ii} + C9—H9*B*···N1^{ii} + C8—H8···C11^{iii}	8.70	−19.7	−3.5	−98.9	71.0	−65.7
C12—H12···S1^{iv}	7.96	−11.1	−1.9	−43.0	33.7	−29.7
H6···H16*B*^{v}	14.23	−0.6	−0.2	−6.7	3.0	−4.8
Inter-layer region						
H5···H14^{vi}	12.44	−10.3	−2.1	−28.1	20.0	−24.6
H16*A*···H16*B*^{vii}	15.29	−1.5	−0.4	−11.8	3.5	−10.0
H6···H14^{viii}	14.93	−3.4	−0.5	−13.6	10.2	−9.5
H6···H16*C*^{ix}	15.43	−1.8	−0.4	−10.9	6.2	−7.8
H6···H7^{x}	21.02	−1.2	−0.2	−7.8	5.4	−4.9

Notes: Symmetry operations: (i) $-x+\frac{1}{2}, y-\frac{1}{2}, z$; (ii) $-x+\frac{1}{2}, y+\frac{1}{2}, z$; (iii) $x-\frac{1}{2}, y-\frac{1}{2}, -z+\frac{3}{2}$; (iv) $-x+1, y+1, -z+\frac{3}{2}$; (v) $x-\frac{1}{2}, y-\frac{3}{2}, -z+\frac{3}{2}$; (vi) $x, -y+1, z+\frac{1}{2}$; (vii) $x, -y+2, z+\frac{1}{2}$; (viii) $-x+\frac{1}{2}, -y+\frac{1}{2}, z+\frac{1}{2}$; (ix) $x+\frac{1}{2}, -y+\frac{3}{2}, -z+1$; (*x*) $-x, -y, -z+2$

5. Computational chemistry

In the present analysis, the pairwise interaction energies between the molecules in the crystal of (I) were calculated by employing the 6-31G(*d*,*p*) basis set with the B3LYP function. The total energy comprises four terms: *i.e.* the electrostatic (E_{ele}), polarization (E_{pol}), dispersion (E_{dis}) and exchange-

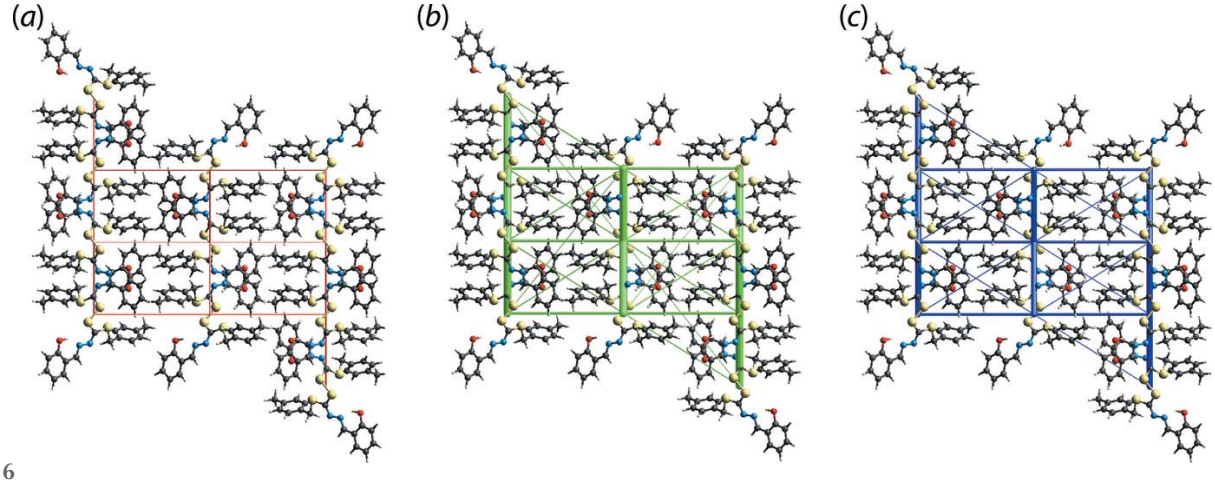

Figure 6
Perspective views of the energy frameworks calculated for (I) showing (*a*) electrostatic potential force, (*b*) dispersion force and (*c*) total energy, each plotted down the *b* axis. The radii of the cylinders are proportional to the relative magnitudes of the corresponding energies and were adjusted to the same scale factor of 55 with a cut-off value of 5 kJ mol^{-1}.

Table 5
A comparison of key geometric parameters (Å, °) in structures related to (I).

Compound	Symmetry	S—S	C—S—S—C	Refcode	Ref.
(I)	2	2.0439 (8)	90.70 (8)	–	This work
(II)	–	2.0386 (7)	88.73 (9)	MUYRIJ	Madanhire *et al.* (2015)
(III)	2	2.0443 (7)	104.67 (8)	DIBYOF01	Yekke-ghasemi *et al.* (2018)
(IV)	–	2.0373 (4)	91.54 (6)	LAGLUD	Islam *et al.* (2016)
(V)	2	2.0504 (7)	96.2 (1)	CUHHET	How *et al.* (2009)

repulsion (E_{rep}) energies and these were calculated in *Crystal Explorer 17* (Turner *et al.*, 2017). The characteristics of the calculated intermolecular interaction energies are summarized in Table 4. As postulated, in the absence of conventional hydrogen bonding in the crystal, the E_{dis} energy term makes the major contribution to the interaction energies. The greatest stabilization energy (–65.7 kJ mol^{-1}) occurs within the intra-layer region and arises from the combination of C—H···π, C···O and C···C short contacts as well as weak C—H···N/C interactions. The second most significant energy of stabilization within the intra-layer region involves a major contribution from the tolyl-C12—H12···S1(sulfanyl) interaction (dominated by E_{dis}) with a total energy of −29.7 kJ mol^{-1}. In addition, a long-range H6···H16*B* contact is observed within the intra-layer region with a H···H separation of 2.44 Å.

The E_{dis} energy term also makes the major contribution to the energies of stabilization in the inter-layer region, with the separation between molecules in the inter-layer region being H···H contacts. The maximum energy is not found for the shortest H6···H14 contact (–9.5 kJ mol^{-1}), Table 2, but rather a pair of phenol-H5···H14(tolyl) contacts (–24.6 kJ mol^{-1}), each with a distance of 2.51 Å. Views of the energy framework diagrams down the *b* axis are shown in Fig. 6 and emphasize the importance of E_{dis} in the stabilization of the crystal.

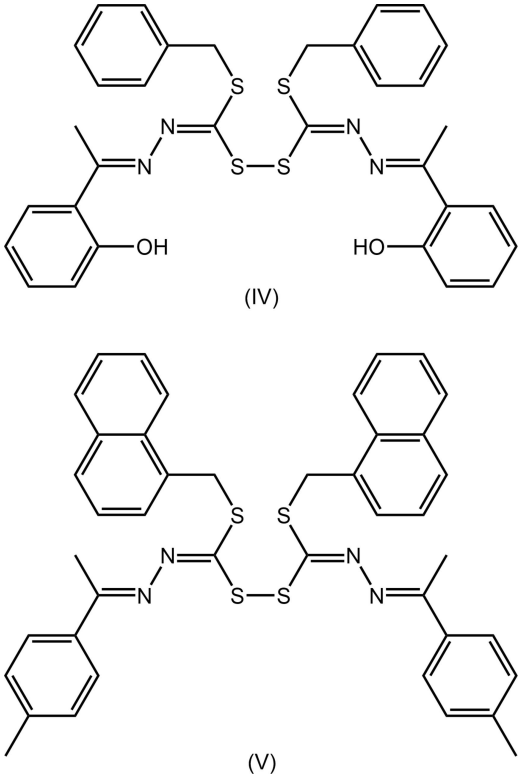

Figure 7
Chemical diagrams for (IV) and (V).

6. Database survey

In the crystallographic literature, there are four precedents for (I) with details collated in Table 5. Derivatives (II) and (III) are most closely related to (I), differing only in the nature of the S-bound *R* group, *i.e.* *R* = Me (MUYRIJ; Madanhire *et al.*, 2015) and *R* = Et (DIBYOF01; Yekke-ghasemi *et al.*, 2018), respectively. As shown in Fig. 7, (IV) is an *S*-benzyl ester with a methyl group on the imine-C atom as well as having the 2-hydroxylbenzene ring (LAGLUD; Islam *et al.*, 2016) whereas (V) is an *S*-methylnaphthyl ester with methyl and 2-tolyl groups bound to the imine-C atom (CUHHET; How *et al.*, 2009). In common with (I), the complete molecules of (III) and (V) are generated by crystallographically imposed twofold symmetry. While lacking this symmetry, (II) and (IV) approximate twofold symmetry as seen in the overlay diagram of Fig. 8, from which is observed that to a first approximation, all five molecules adopt a similar conformation. The S—S bond length in (I) lies between the experimentally distinct

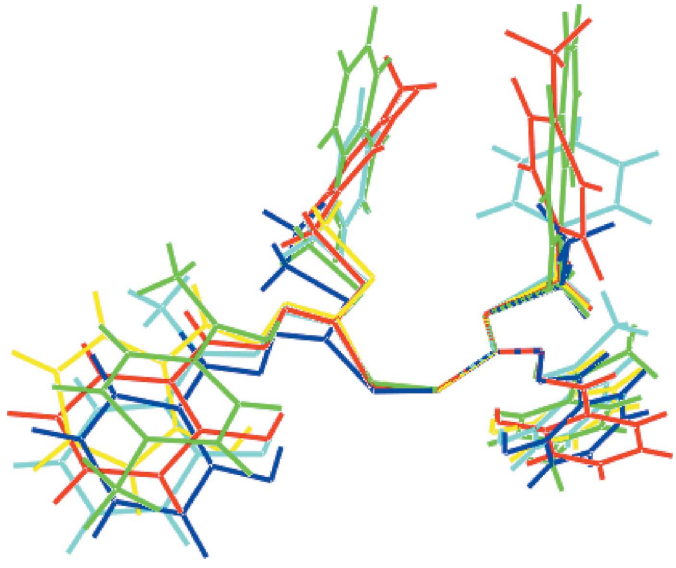

Figure 8
An overlay diagram of (I) red image, (II) yellow, (III) blue, (IV) aqua and (V) green. The molecules have been overlapped so a CS_2 residue of each molecule is coincident.

Table 6
Experimental details.

Crystal data	
Chemical formula	$C_{32}H_{30}N_4O_2S_4$
M_r	630.84
Crystal system, space group	Orthorhombic, *Pbcn*
Temperature (K)	100
a, *b*, *c* (Å)	15.4653 (4), 7.9639 (2), 24.8116 (7)
V (Å^3)	3055.90 (14)
Z	4
Radiation type	Cu *Kα*
μ (mm^{-1})	3.15
Crystal size (mm)	0.27 × 0.14 × 0.07
Data collection	
Diffractometer	Agilent Xcalibur, Eos, Gemini
Absorption correction	Multi-scan (*CrysAlis PRO*; Agilent, 2012)
T_{min}, T_{max}	0.819, 1.000
No. of measured, independent and observed [$I > 2\sigma(I)$] reflections	10206, 2933, 2637
R_{int}	0.022
(sin $\theta/\lambda)_{max}$ (Å^{-1})	0.614
Refinement	
$R[F^2 > 2\sigma(F^2)]$, $wR(F^2)$, *S*	0.038, 0.102, 1.04
No. of reflections	2933
No. of parameters	194
No. of restraints	1
H-atom treatment	H atoms treated by a mixture of independent and constrained refinement
$\Delta\rho_{max}$, $\Delta\rho_{min}$ (e Å^{-3})	0.45, −0.20

Computer programs: *CrysAlis PRO* (Agilent, 2012), *SHELXT2014/4* (Sheldrick, 2015*a*), *SHELXL2018/3* (Sheldrick, 2015*b*), *ORTEP-3 for Windows* (Farrugia, 2012), *DIAMOND* (Brandenburg, 2006) and *publCIF* (Westrip, 2010).

range of 2.0373 (4) Å in (IV) and 2.0504 (7) Å in (V). In the same way, the C—S—S—C torsion angle in (I) lies between the extreme values of 88.73 (6) and 104.67 (8)° in (II) and (III), respectively.

7. Synthesis and crystallization

Crystals of (I) were isolated from an ethanol–acetonitrile solution by slow evaporation and was a side-product from the synthesis of the Schiff base 4-methylbenzyl-2-(2-hydroxybenzylidene) hydrazinecarbodithioate carried out by heating a mixture of *S*-4-methylbenzyldithiocarbazate (10 mmol) and salicylaldehyde (10 mmol) in ∼30 ml of acetonitrile for about 2 h (Ravoof *et al.*, 2010). Slow evaporation of the remaining filtrate after removal of the desired product over a period of several days gave yellow plates of (I).

8. Refinement

Crystal data, data collection and structure refinement details are summarized in Table 6. The carbon-bound H atoms were placed in calculated positions (C—H = 0.95–0.99 Å) and were included in the refinement in the riding-model approximation, with U_{iso}(H) set to 1.2U_{eq}(C). The O-bound H atom was located in a difference-Fourier map, but was refined with an O—H = 0.84±0.01 Å distance restraint, and with U_{iso}(H) set to 1.5U_{eq}(O).

Acknowledgements

The intensity data were collected by Mohamed I. M. Tahir, Universiti Putra Malaysia.

Funding information

Crystallographic research at Sunway University is supported by Sunway University Sdn Bhd (grant No. STR-RCTR-RCCM-001–2019).

References

Agilent (2012). *CrysAlis PRO*. Agilent Technologies, Yarnton, England.
Amirnasr, M., Bagheri, M., Farrokhpour, H., Schenk, K. J., Mereiter, K. & Ford, P. C. (2014). *Polyhedron*, **71**, 1–7.
Brandenburg, K. (2006). *DIAMOND*. Crystal Impact GbR, Bonn, Germany.
Farrugia, L. J. (2012). *J. Appl. Cryst.* **45**, 849–854.
How, F. N.-F., Crouse, K. A., Tahir, M. I. M. & Watkin, D. J. (2009). *J. Chem. Crystallogr.* **39**, 894–897.
Islam, M. A. A. A. A., Sheikh, M. C., Islam, M. H., Miyatake, R. & Zangrando, E. (2016). *Acta Cryst.* E**72**, 337–339.
Low, M. L., Maigre, L. M., Tahir, M. I. M. T., Tiekink, E. R. T., Dorlet, P., Guillot, R., Ravoof, T. B., Rosli, R., Pagès, J.-M., Policar, C., Delsuc, N. & Crouse, K. A. (2016). *Eur. J. Med. Chem.* **120**, 1–12.
Madanhire, T., Abrahams, A., Hosten, E. C. & Betz, R. (2015). *Z. Kristallogr. New Cryst. Struct.* **230**, 89–90.
Ravoof, T. B. S. A., Crouse, K. A., Tahir, M. I. M., How, F. N. F., Rosli, R. & Watkins, D. J. (2010). *Transition Met. Chem.* **35**, 871–876.
Ravoof, T. B. S. A., Crouse, K. A., Tiekink, E. R. T., Tahir, M. I. M., Yusof, E. N. M. & Rosli, R. (2017). *Polyhedron*, **133**, 383–392.
Sheldrick, G. M. (2015*a*). *Acta Cryst.* A**71**, 3–8.
Sheldrick, G. M. (2015*b*). *Acta Cryst.* C**71**, 3–8.
Sohtun, W. P., Kannan, A., Krishna, K. H., Saravanan, D., Kumar, M. S. & Velusamy, M. (2018). *Acta Chim. Slov.* **65**, 621–629.
Spek, A. L. (2020). *Acta Cryst.* E**76**, 1–11.
Tan, S. L., Jotani, M. M. & Tiekink, E. R. T. (2019). *Acta Cryst.* E**75**, 308–318.
Turner, M. J., Mckinnon, J. J., Wolff, S. K., Grimwood, D. J., Spackman, P. R., Jayatilaka, D. & Spackman, M. A. (2017). *Crystal Explorer 17*. The University of Western Australia.
Westrip, S. P. (2010). *J. Appl. Cryst.* **43**, 920–925.
Yekke-ghasemi, Z., Takjoo, R., Ramezani, M. & Mague, J. T. (2018). *RSC Adv.* **8**, 41795–41809.
Yusof, E. N. M., Ishak, N. N. M., Latif, M. A. M., Tahir, M. I. M., Sakoff, J. A., Page, A. J., Tiekink, E. R. T. & Ravoof, T. B. S. A. (2020). *Res. Chem. Intermed.* **46**, 2351–2379.

supporting information

Acta Cryst. (2020). E**76**, 1245-1250 [https://doi.org/10.1107/S2056989020008762]

2-[(1*E*)-[(*Z*)-2-({[(1*Z*)-[(*E*)-2-[(2-Hydroxyphenyl)methylidene]hydrazin-1-ylidene]({[(4-methylphenyl)methyl]sulfanyl})methyl]disulfanyl}({[(4-methylphenyl)-methyl]sulfanyl})methylidene)hydrazin-1-ylidene]methyl]phenol: crystal structure, Hirshfeld surface analysis and computational study

Georgiana Paulus, Huey Chong Kwong, Karen A. Crouse and Edward R. T. Tiekink

Computing details

Data collection: *CrysAlis PRO* (Agilent, 2012); cell refinement: *CrysAlis PRO* (Agilent, 2012); data reduction: *CrysAlis PRO* (Agilent, 2012); program(s) used to solve structure: *SHELXT2014/4* (Sheldrick, 2015*a*); program(s) used to refine structure: *SHELXL2018/3* (Sheldrick, 2015*b*); molecular graphics: *ORTEP-3 for Windows* (Farrugia, 2012) and *DIAMOND* (Brandenburg, 2006); software used to prepare material for publication: *publCIF* (Westrip, 2010).

2-[(1*E*)-[(*Z*)-2-({[(1*Z*)-[(*E*)-2-[(2-Hydroxyphenyl)methylidene]hydrazin-1-ylidene]({[(4-methylphenyl)methyl]sulfanyl})methyl]disulfanyl}({[(4-methylphenyl)methyl]sulfanyl})methylidene)hydrazin-1-ylidene]methyl]phenol

Crystal data

$C_{32}H_{30}N_4O_2S_4$
$M_r = 630.84$
Orthorhombic, *Pbcn*
$a = 15.4653$ (4) Å
$b = 7.9639$ (2) Å
$c = 24.8116$ (7) Å
$V = 3055.90$ (14) Å^3
$Z = 4$
$F(000) = 1320$
$D_x = 1.371$ Mg m^{-3}
Cu $K\alpha$ radiation, $\lambda = 1.54178$ Å
Cell parameters from 4566 reflections
$\theta = 3.4$–$71.1°$
$\mu = 3.15$ mm^{-1}
$T = 100$ K
Plate, yellow
0.27 × 0.14 × 0.07 mm

Data collection

Agilent Xcalibur, Eos, Gemini diffractometer
Radiation source: Enhance (Cu) X-ray Source
Graphite monochromator
Detector resolution: 16.1952 pixels mm^{-1}
ω scans
Absorption correction: multi-scan (CrysAlisPro; Agilent, 2012)
$T_{min} = 0.819$, $T_{max} = 1.000$
10206 measured reflections
2933 independent reflections
2637 reflections with $I > 2\sigma(I)$
$R_{int} = 0.022$
$\theta_{max} = 71.3°$, $\theta_{min} = 3.6°$
$h = -18 \rightarrow 18$
$k = -7 \rightarrow 9$
$l = -29 \rightarrow 30$

Refinement

Refinement on F^2
Least-squares matrix: full
$R[F^2 > 2\sigma(F^2)] = 0.038$
$wR(F^2) = 0.102$
$S = 1.04$
2933 reflections
194 parameters
1 restraint
Primary atom site location: dual
Secondary atom site location: difference Fourier map
Hydrogen site location: mixed
H atoms treated by a mixture of independent and constrained refinement
$w = 1/[\sigma^2(F_o^2) + (0.0662P)^2 + 1.2702P]$ where $P = (F_o^2 + 2F_c^2)/3$
$(\Delta/\sigma)_{max} = 0.001$
$\Delta\rho_{max} = 0.45$ e Å^{-3}
$\Delta\rho_{min} = -0.20$ e Å^{-3}

Special details

Geometry. All esds (except the esd in the dihedral angle between two l.s. planes) are estimated using the full covariance matrix. The cell esds are taken into account individually in the estimation of esds in distances, angles and torsion angles; correlations between esds in cell parameters are only used when they are defined by crystal symmetry. An approximate (isotropic) treatment of cell esds is used for estimating esds involving l.s. planes.

Fractional atomic coordinates and isotropic or equivalent isotropic displacement parameters (Å^2)

	x	y	z	U_{iso}*/U_{eq}
S1	0.44788 (3)	0.20945 (5)	0.77532 (2)	0.02123 (14)
S2	0.41121 (3)	0.47744 (6)	0.69155 (2)	0.02165 (14)
O1	0.32052 (8)	0.08476 (16)	0.89877 (5)	0.0239 (3)
H1O	0.3312 (16)	0.141 (3)	0.8711 (7)	0.036*
N1	0.30058 (9)	0.38409 (19)	0.76780 (6)	0.0210 (3)
N2	0.28689 (10)	0.28083 (18)	0.81313 (6)	0.0200 (3)
C1	0.37582 (11)	0.3625 (2)	0.74728 (7)	0.0188 (3)
C2	0.20696 (11)	0.2752 (2)	0.82727 (7)	0.0208 (4)
H2	0.166079	0.339978	0.807651	0.025*
C3	0.17688 (11)	0.1739 (2)	0.87198 (7)	0.0202 (3)
C4	0.23359 (11)	0.0816 (2)	0.90530 (7)	0.0197 (3)
C5	0.19995 (12)	−0.0185 (2)	0.94637 (7)	0.0221 (4)
H5	0.237862	−0.080587	0.968950	0.027*
C6	0.11138 (13)	−0.0276 (2)	0.95434 (7)	0.0246 (4)
H6	0.089111	−0.097226	0.982149	0.029*
C7	0.05458 (11)	0.0638 (3)	0.92221 (7)	0.0259 (4)
H7	−0.006038	0.057531	0.928079	0.031*
C8	0.08769 (11)	0.1640 (2)	0.88161 (7)	0.0236 (4)
H8	0.049188	0.227355	0.859785	0.028*
C9	0.31721 (11)	0.6135 (2)	0.68128 (7)	0.0241 (4)
H9A	0.268116	0.547317	0.666962	0.029*
H9B	0.299350	0.664563	0.715912	0.029*
C10	0.34232 (11)	0.7481 (2)	0.64183 (7)	0.0206 (4)
C11	0.38760 (12)	0.8900 (2)	0.65887 (7)	0.0249 (4)
H11	0.402651	0.901799	0.695798	0.030*
C12	0.41082 (12)	1.0139 (2)	0.62245 (8)	0.0265 (4)
H12	0.441428	1.109823	0.634869	0.032*
C13	0.39015 (12)	1.0006 (2)	0.56792 (8)	0.0246 (4)

C14	0.34520 (12)	0.8595 (2)	0.55108 (7)	0.0252 (4)
H14	0.330262	0.848022	0.514124	0.030*
C15	0.32150 (12)	0.7340 (2)	0.58738 (7)	0.0234 (4)
H15	0.290918	0.638161	0.574895	0.028*
C16	0.41484 (14)	1.1379 (3)	0.52889 (9)	0.0370 (5)
H16A	0.408036	1.097062	0.491877	0.056*
H16B	0.475189	1.170350	0.534944	0.056*
H16C	0.377305	1.235519	0.534517	0.056*

Atomic displacement parameters (Å²)

	U^{11}	U^{22}	U^{33}	U^{12}	U^{13}	U^{23}
S1	0.0191 (2)	0.0229 (2)	0.0217 (2)	0.00008 (15)	0.00049 (14)	0.00357 (16)
S2	0.0204 (2)	0.0248 (2)	0.0197 (2)	0.00156 (16)	0.00321 (15)	0.00481 (16)
O1	0.0191 (6)	0.0272 (7)	0.0254 (6)	0.0013 (5)	0.0003 (5)	0.0051 (5)
N1	0.0216 (7)	0.0242 (7)	0.0173 (7)	−0.0009 (6)	−0.0002 (5)	0.0020 (6)
N2	0.0213 (7)	0.0223 (8)	0.0163 (7)	−0.0009 (6)	0.0004 (5)	0.0009 (5)
C1	0.0200 (8)	0.0198 (8)	0.0167 (8)	−0.0019 (6)	−0.0017 (6)	−0.0001 (6)
C2	0.0207 (8)	0.0227 (9)	0.0189 (8)	0.0017 (7)	−0.0024 (6)	−0.0021 (6)
C3	0.0224 (8)	0.0215 (8)	0.0168 (8)	−0.0005 (7)	0.0009 (6)	−0.0035 (7)
C4	0.0200 (8)	0.0199 (8)	0.0191 (8)	−0.0021 (7)	0.0011 (6)	−0.0045 (6)
C5	0.0266 (9)	0.0214 (9)	0.0182 (8)	−0.0001 (7)	−0.0008 (7)	−0.0015 (6)
C6	0.0299 (10)	0.0249 (9)	0.0189 (8)	−0.0053 (7)	0.0059 (7)	−0.0022 (7)
C7	0.0194 (9)	0.0343 (10)	0.0239 (9)	−0.0033 (7)	0.0029 (7)	−0.0041 (8)
C8	0.0204 (9)	0.0295 (9)	0.0211 (9)	0.0005 (7)	−0.0010 (6)	−0.0021 (7)
C9	0.0179 (8)	0.0283 (9)	0.0261 (9)	0.0034 (7)	0.0009 (7)	0.0069 (7)
C10	0.0170 (8)	0.0223 (8)	0.0226 (9)	0.0041 (6)	0.0009 (6)	0.0024 (7)
C11	0.0252 (9)	0.0282 (9)	0.0215 (9)	0.0031 (7)	−0.0033 (7)	−0.0024 (7)
C12	0.0234 (9)	0.0215 (9)	0.0347 (11)	−0.0020 (7)	−0.0059 (7)	−0.0020 (7)
C13	0.0205 (8)	0.0234 (9)	0.0299 (10)	0.0023 (7)	0.0004 (7)	0.0066 (7)
C14	0.0288 (9)	0.0275 (9)	0.0193 (8)	0.0027 (7)	−0.0031 (7)	0.0009 (7)
C15	0.0240 (9)	0.0208 (8)	0.0254 (9)	−0.0014 (7)	−0.0041 (7)	−0.0008 (7)
C16	0.0354 (11)	0.0336 (11)	0.0420 (12)	−0.0050 (9)	0.0003 (9)	0.0133 (9)

Geometric parameters (Å, º)

S1—C1	1.7921 (17)	C7—H7	0.9500
S1—S1^{i}	2.0439 (8)	C8—H8	0.9500
S2—C1	1.7463 (17)	C9—C10	1.503 (2)
S2—C9	1.8308 (18)	C9—H9A	0.9900
O1—C4	1.354 (2)	C9—H9B	0.9900
O1—H1O	0.839 (10)	C10—C15	1.393 (2)
N1—C1	1.282 (2)	C10—C11	1.395 (3)
N1—N2	1.409 (2)	C11—C12	1.385 (3)
N2—C2	1.286 (2)	C11—H11	0.9500
C2—C3	1.448 (2)	C12—C13	1.394 (3)
C2—H2	0.9500	C12—H12	0.9500
C3—C8	1.402 (2)	C13—C14	1.386 (3)

C3—C4	1.412 (2)	C13—C16	1.510 (3)
C4—C5	1.394 (2)	C14—C15	1.394 (3)
C5—C6	1.386 (3)	C14—H14	0.9500
C5—H5	0.9500	C15—H15	0.9500
C6—C7	1.392 (3)	C16—H16A	0.9800
C6—H6	0.9500	C16—H16B	0.9800
C7—C8	1.383 (3)	C16—H16C	0.9800

C1—S1—S1^{i}	104.58 (6)	C10—C9—H9A	110.1
C1—S2—C9	99.87 (8)	S2—C9—H9A	110.1
C4—O1—H1O	107.7 (17)	C10—C9—H9B	110.1
C1—N1—N2	112.04 (14)	S2—C9—H9B	110.1
C2—N2—N1	112.49 (14)	H9A—C9—H9B	108.4
N1—C1—S2	121.92 (13)	C15—C10—C11	118.36 (16)
N1—C1—S1	120.10 (13)	C15—C10—C9	120.95 (16)
S2—C1—S1	117.98 (10)	C11—C10—C9	120.68 (16)
N2—C2—C3	122.48 (16)	C12—C11—C10	120.62 (17)
N2—C2—H2	118.8	C12—C11—H11	119.7
C3—C2—H2	118.8	C10—C11—H11	119.7
C8—C3—C4	118.81 (16)	C11—C12—C13	121.29 (17)
C8—C3—C2	118.54 (16)	C11—C12—H12	119.4
C4—C3—C2	122.63 (16)	C13—C12—H12	119.4
O1—C4—C5	117.93 (16)	C14—C13—C12	117.98 (17)
O1—C4—C3	122.47 (15)	C14—C13—C16	121.39 (18)
C5—C4—C3	119.59 (16)	C12—C13—C16	120.62 (18)
C6—C5—C4	120.20 (17)	C13—C14—C15	121.21 (17)
C6—C5—H5	119.9	C13—C14—H14	119.4
C4—C5—H5	119.9	C15—C14—H14	119.4
C5—C6—C7	120.98 (17)	C10—C15—C14	120.53 (17)
C5—C6—H6	119.5	C10—C15—H15	119.7
C7—C6—H6	119.5	C14—C15—H15	119.7
C8—C7—C6	119.01 (17)	C13—C16—H16A	109.5
C8—C7—H7	120.5	C13—C16—H16B	109.5
C6—C7—H7	120.5	H16A—C16—H16B	109.5
C7—C8—C3	121.39 (17)	C13—C16—H16C	109.5
C7—C8—H8	119.3	H16A—C16—H16C	109.5
C3—C8—H8	119.3	H16B—C16—H16C	109.5
C10—C9—S2	107.91 (12)		

C1—N1—N2—C2	−166.57 (15)	C5—C6—C7—C8	0.4 (3)
N2—N1—C1—S2	−178.60 (11)	C6—C7—C8—C3	0.6 (3)
N2—N1—C1—S1	2.0 (2)	C4—C3—C8—C7	−1.2 (3)
C9—S2—C1—N1	2.05 (17)	C2—C3—C8—C7	177.24 (16)
C9—S2—C1—S1	−178.53 (10)	C1—S2—C9—C10	168.30 (13)
S1^{i}—S1—C1—N1	174.92 (13)	S2—C9—C10—C15	97.92 (17)
S1^{i}—S1—C1—S2	−4.51 (11)	S2—C9—C10—C11	−81.68 (18)
N1—N2—C2—C3	178.45 (15)	C15—C10—C11—C12	0.3 (3)
N2—C2—C3—C8	−174.53 (17)	C9—C10—C11—C12	179.90 (16)

N2—C2—C3—C4	3.8 (3)	C10—C11—C12—C13	−0.3 (3)
C8—C3—C4—O1	−179.81 (15)	C11—C12—C13—C14	0.2 (3)
C2—C3—C4—O1	1.8 (3)	C11—C12—C13—C16	179.13 (18)
C8—C3—C4—C5	0.8 (3)	C12—C13—C14—C15	−0.2 (3)
C2—C3—C4—C5	−177.54 (16)	C16—C13—C14—C15	−179.12 (18)
O1—C4—C5—C6	−179.26 (15)	C11—C10—C15—C14	−0.3 (3)
C3—C4—C5—C6	0.2 (3)	C9—C10—C15—C14	−179.90 (16)
C4—C5—C6—C7	−0.8 (3)	C13—C14—C15—C10	0.3 (3)

Symmetry code: (i) −*x*+1, *y*, −*z*+3/2.

Hydrogen-bond geometry (Å, º)

*Cg*1 is the centroid of the (C10–C15) ring.

D—H···*A*	*D*—H	H···*A*	*D*···*A*	*D*—H···*A*
O1—H1*O*···N2	0.84 (2)	1.94 (2)	2.6877 (19)	148 (2)
C9—H9*A*···*Cg*1^{ii}	0.99	2.93	3.9075 (18)	169

Symmetry code: (ii) *x*, −*y*−1, *z*−1/2.